Available online at www.sciencedirect.com

jmr&t Journal of Materials Research and Technology

www.jmrt.com.br

Original Article

Electronic and ionic conductivity studies on microwave synthesized glasses containing transition metal ions

Basareddy Sujatha[a], *Ramarao Viswanatha*[b], *Hanumathappa Nagabushana*[c], *Chinnappa Narayana Reddy*[d,*]

[a] *Department of Electronics & Communication, MSR Institute of Technology, Bangalore, India*
[b] *Solid State and Structural Chemistry Unit, Indian Institute of Science, Bangalore, India*
[c] *Department of Physics, Tumkur University, Tumkur, India*
[d] *Department of Physics, Sree Siddaganga College of Arts, Science and Commerce, Tumkur University, Tumkur, India*

ARTICLE INFO

Article history:
Received 27 April 2015
Accepted 8 March 2016
Available online 15 April 2016

Keywords:
Microwave synthesis
Semiconducting
Modulated DSC
Impedance
EPR study

ABSTRACT

Glasses in the system $xV_2O_5{\cdot}20Li_2O{\cdot}(80-x)$ [$0.6B_2O_3{:}0.4ZnO$] (where $10 \leq x \leq 50$) have been prepared by a simple microwave method. Microwave synthesis of materials offers advantages of efficient transformation of energy throughout the volume in an effectively short time. Conductivity in these glasses was controlled by the concentration of transition metal ion (TMI). The dc conductivity follows Arrhenius law and the activation energies determined by regression analysis varies with the content of V_2O_5 in a non-linear passion. This non-linearity is due to different conduction mechanisms operating in the investigated glasses. Impedance and electron paramagnetic resonance (EPR) spectroscopic studies were performed to elucidate the nature of conduction mechanism. Cole–cole plots of the investigated glasses consist of (i) single semicircle with a low frequency spur, (ii) two depressed semicircles and (iii) single semicircle without spur, which suggests the operation of two conduction mechanisms. EPR spectra reveal the existence of electronic conduction between aliovalent vanadium sites. Further, in highly modified ($10V_2O_5$ mol%) glasses Li^+ ion migration dominates.

1. Introduction

The conductivity in glasses has been of interest for long time because of their potential technological applications. Use of glasses as electrolyte and electrode materials has given a boost to the study of ion transport in glasses and search for new glassy materials [1–5]. The mechanism of electrical conductivity in ion-electron conducting glasses is a challenging problem [5–8].

* *Corresponding author.*
E-mail: nivetejareddy@gmail.com (C. Narayana Reddy).
http://dx.doi.org/10.1016/j.jmrt.2016.03.002

In recent years many glassy materials have been synthesized as binary or ternary systems using network forming oxides such as B_2O_3, P_2O_5, TeO_2 etc and alkali or silver oxides as modifiers by melt quenching method [1]. Microwave synthesis of materials is a new technology undergoing rapid developments due to potential advantages it offers such as reduced processing time, energy efficiency and products with enhanced properties. The only requirement of this method is that at least one of the components used for synthesizing materials should be a microwave susceptor [1,2].

Alkali borate glasses have been extensively studied over the past two decades to elucidate the nature and relative concentration of various borate units constituting the glass network [9]. B^{3+} atoms in these glasses are both in trigonal and tetrahedral state. The concentration of these borate species in the glass structure is however determined by the nature and the content of the modifier oxide. In glasses containing B_2O_3 and V_2O_5 the coordination number and connectivities of both borate and vanadate species vary in a complex manner as a consequence of modification [9]. Further, modification is understood to be the reaction of oxide ion (O^{2-}), which results in structural changes, by creating non-bridging oxygens (NBOs). These NBOs constitutes anionic sites with different binding energies in comparison to those oxygens localized in boron tetrahedra [1]. Horopanitis et al. [10] pointed out that, the Li^+ transport in lithiated boron oxide glasses increases with Li_2O concentration, not only due to Li^+ ion concentration but also due to structural modification. Ion conducting glasses with high $Li^+/Na^+/Ag^+/Cu^+$ concentration are called fast ion conductors (FIC) and they are promising glassy electrolyte for the solid state batteries [5,11,12].

Glasses containing transition metal oxide (TMO) such as V_2O_5, Fe_2O_3, CuO, MoO_3, WO_3, CoO, etc. are known to exhibit semiconducting property and hence these glasses have been studied extensively from the cathode point of view of batteries [1,13]. The existence of relative proportions of low and high valence states of transition metal ions (TMIs) is responsible for the electronic conduction in these glasses [6,14]. It is expected that TMO added to alkali modified glass, results in mixed conduction [6,15,16].

EPR spectra of V_2O_5 containing glasses originate from V^{4+} paramagnetic centers whose outer electronic structure $3p^6$, $3d^1$ enables unpaired magnetic moments of $3d^1$ electrons to interact with the electromagnetic field in the microwave range. Whereas, the electronic structure of V^{5+} is $3p^6$, which has total electron spin zero. Since the V^{4+} ion has electronic spin $s = 1/2$ and nuclear spin of ^{51}V is $I = 7/2$, one should expect interactions between corresponding magnetic moments resulting in the hyperfine structure [17]. Gupta et al. [18] pointed out that, long range electron spin–spin interactions between V^{4+} ions and the spin–orbit coupling cause an anisotropy of the g-factor and the broadening of the individual lines. In glasses, only orientation averaged spectra can be observed, which can lead to additional reduction of hyperfine structure lines. It was seen in V_2O_5–TeO_2 glasses that the disappearance of hyperfine structure lines at higher contents of V_2O_5 is due to super-exchange interaction of V^{4+}—O—V^{5+} chains [18]. In this study we used impedance and EPR spectroscopic studies to analyze conduction mechanisms in microwave synthesized $xV_2O_5{\cdot}20Li_2O{\cdot}(80-x)$ [$0.6B_2O_3$:0.4ZnO] glasses.

2. Experimental

Glasses were prepared by microwave heating technique using $xV_2O_5{\cdot}20Li_2O{\cdot}(80-x)$ [$0.6B_2O_3$:0.4ZnO] (where $10 < x < 50$) glass system. Analar grade vanadium pentoxide (V_2O_5) lithium carbonate (Li_2CO_3), orthoboric acid (H_3BO_3) and zinc oxide (ZnO) were used as starting materials. An appropriate quantity of weighed chemicals were mixed and thoroughly ground to homogenize the mixture and kept in a silica crucible inside a domestic microwave oven operating at 2.45 GHz and at a tunable power level up to a maximum of 850 W. When microwaves were switched on, complete decomposition of H_3BO_3 to B_2O_3, water and Li_2CO_3 to Li_2O, carbon dioxide was achieved in 2–3 min. Within 6–8 min of microwave exposure a good homogeneous melt was obtained, which was immediately quenched between brass blocks. The silica crucible was found to remain clean and unaffected during the short duration of melting. The glass was annealed in a muffle furnace for 1 h at 150 °C to remove thermal strains that could have developed during quenching. The samples were preserved in a sealed desiccator containing $CaCl_2$.

Glass transition temperature (T_g) of the samples was extracted from the thermograms recorded using Differential Scanning Colorimeter (Perkin Elmer DSC-2). For the electrical measurements, the annealed samples were thoroughly polished and coated with silver paste on both sides, which serve as electrodes having a thickness of about 0.1 cm and diameter of about 0.8 cm were used. The resistance of the sample was calculated by applying a dc field of 2 V and measuring the current through it using a digital electrometer (ECIL EA-5600). The conductivity of the sample was calculated using the relation:

$$\sigma_{dc} = \frac{d}{RA} \tag{1}$$

where d is the thickness of the sample and A is the area of the sample. Temperatures of the samples were measured using a chromel–alumel thermocouple placed very close to the sample holder. The measurements were repeated with changed polarity of the applied voltages.

Capacitance (C_p) and conductance (G) of the samples were measured as a function of frequency using a Hewlett-Packard HP 4192A impedance-gain phase analyzer from 100 Hz to 10 MHz in the temperature range 323–405 K. A home built cell assembly (having two terminal capacitor configuration and spring loaded silver electrodes) was used for the measurements. The temperature was controlled using Heatcon (Bangalore 560090, India) temperature controller with an accuracy of ±1 K in the entire range of measurements. The temperature of the sample was measured using Pt-Rh thermocouple positioned very close to the sample.

3. Results and discussion

The X-ray diffraction spectra of the annealed glasses did not show any sharp peaks (Fig. 1), indicating that the samples are

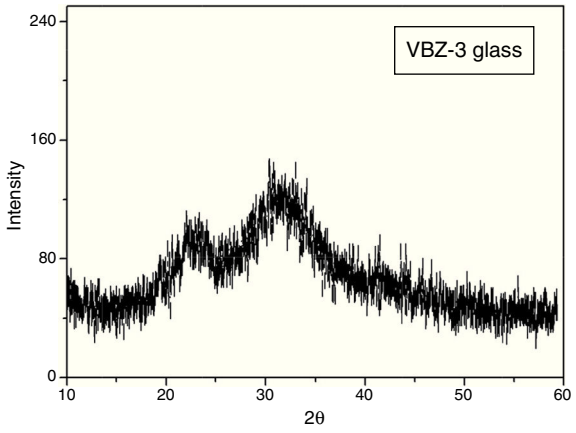

Fig. 1 – A typical XRD spectra of VBZ3 glass.

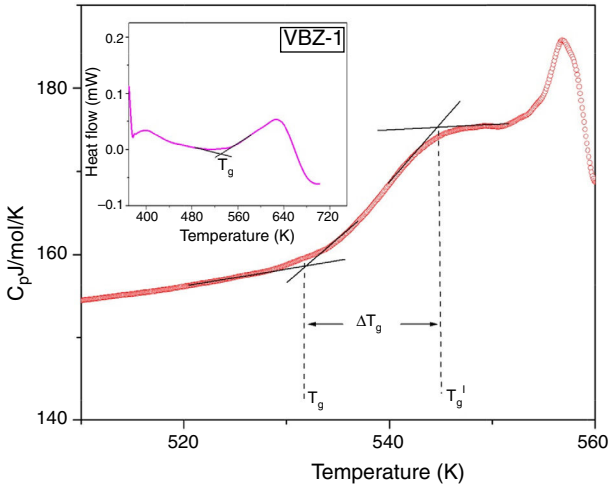

Fig. 2 – Modulated DSC thermogram of VBZ1 glass. Inset: Variation of heat flow with temperature of VBZ1 glass.

amorphous. The method used to extract glass transition temperature (T_g) and liquidus temperature (T_g^{Liquid}) is indicated in the DSC thermograms of heat capacity as shown in Fig. 2. Also, a thermogram of heat flow versus temperature of VBZ-1 glass is shown in Fig. 2 inset. Codes, composition, glass transition temperature (T_g), glass transition width (ΔT_g), activation energy (E_{dc}), are listed in Table 1. The T_gs are decreasing with increasing V_2O_5 mol%. This decrease in T_g can be explained on the basis of the structural changes occur due to network

Table 1 – Code, composition, glass transition temperature (T_g), glass transition width (ΔT_g), activation energy (E_{dc}) of V_2O_5·Li_2O·[0.6B_2O_3:0.4ZnO] glass system.

Code	Composition (mol%)				T_g (K)	ΔT_g (K)	$E_{dc} \pm 0.002$ (eV)
	V_2O_5	Li_2O	B_2O_3	ZnO			
VBZ1	10	20	42	28	531	13.2	0.91
VBZ2	20	20	36	24	527	13.09	0.621
VBZ3	30	20	30	20	524	13.0	0.499
VBZ4	40	20	24	16	519	12.8	0.462
VBZ5	50	20	18	12	513	12.7	0.411

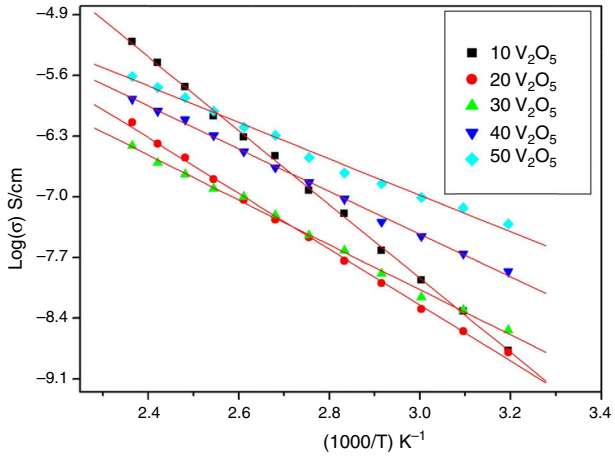

Fig. 3 – Variation of log (σ) versus (1000/T) of xV_2O_5·20Li_2O·(80 – x) [0.6B_2O_3:0.4ZnO] glass system.

modification. A simple borovanadate network consists of a continuous random network formed by $[VOO_{3/2}]^0$ and $[BO_{3/2}]^0$ structural units. Boron is 3-connected and 3-coordinated, while vanadium is 3-connected but 4-coordinated. Therefore, the random network structure consists of B—O—B and B—O—V linkages in B_2O_3 rich glasses while B—O—V and V—O—V linkages are present in V_2O_5 rich glasses. Only B—O—V linkages are expected to be present when the concentrations of these two glass formers (B_2O_3 and V_2O_5) are in equal proportion [19,20]. The variation of T_g with V_2O_5 mol% can be rationalized on the basis of network connectivities, such that, as V_2O_5 increases the stronger B—O—V and B—O—B linkages (bond dissociation energy of B—O is 715 kJ/mol) are replaced by V—O—V linkages (bond dissociation energy of V—O is 617.6 kJ/mol) [19]. Further, the glass transition width ($\Delta T_g = T_g^{Liquid} - T_g$, where T_g^{Liquid} is the liquidus temperature and T_g is glass transition temperature) marginally decreases with increasing V_2O_5 mol%. According to the empirical criterion proposed by Moynihan [21] the glass formers displaying widths $\Delta T_g > 30$ are classified as "Strong" glass and those with $\Delta T_g < 30$ are termed as fragile [22]. As can be seen from Table 1, ΔT_g is much less than 30, hence the investigated glasses are "fragile".

3.1. *DC conductivity by four-probe method*

The dc conductivity of the same composition from different batches prepared under identical conditions showed agreement within 5% error and dc conductivity on the same samples in different runs are within 2% error. Fig. 3 represents the variation of log (σ) as a function of inverse temperature for different V_2O_5 concentrations. It is depicted from Fig. 3 that the conductivity values lie in the range 1.548×10^{-9}–3.784×10^{-6} S/cm when temperature varied from 313 to 423 K. Further, Fig. 3 shows that all the samples follow Arrhenius law:

$$\sigma = \sigma_0 e^{-E_{dc/KT}} \quad (2)$$

and the solid line represents the linear least square fits used to obtain the activation energies (E_{dc}) [23]. Fig. 4

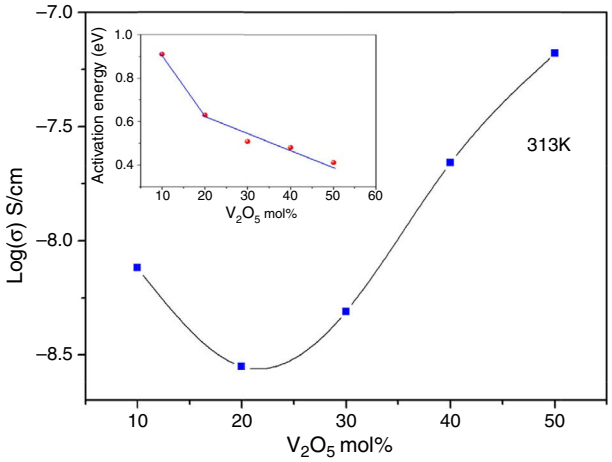

Fig. 4 – Variation of log (σ) with V_2O_5 concentration. Inset: Variation of E_{dc} with V_2O_5 concentration.

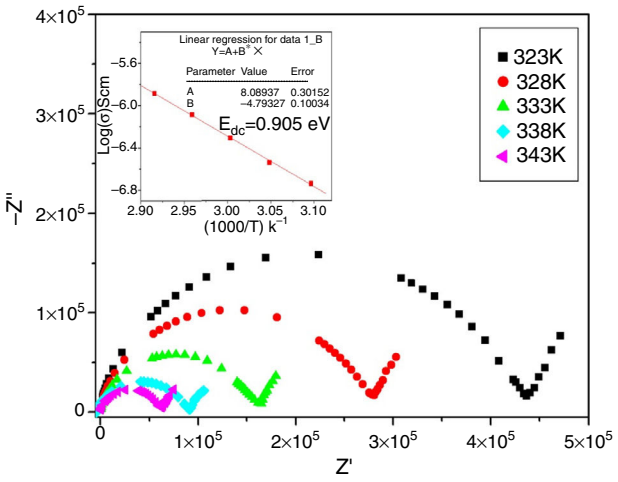

Fig. 5 – Impedance plot of VBZ 1 glass. Inset: Variation of log (σ) versus 1000/T for VBZ1 glass.

shows the variation of log (σ) with V_2O_5 concentration and Fig. 4 inset represents the variation of activation energy (E_{dc}) with V_2O_5 concentration. As can be seen from Fig. 4, the variation is non-linear, indicating that different conducting mechanisms operating in the investigated glasses. Activation energy, $E_{dc} = 0.83 \pm 0.002$ eV for $x = 10$ mol%, which is comparable with those of ion conducting glasses [24,25]. While for $x = 30$–50 mol%, E_{dc} is in the range 0.5 ± 0.002–0.41 ± 0.003 eV. These values are comparable with the activation barriers of electronically conducting glasses [26]. Also, the non-linear variation of activation energy was reported by Garbarczyk et al. [8] and Jozwiak et al. [26] in their studies on silver–vanadate–phosphate and Li_2O–V_2O_5–P_2O_5 glass system, respectively. In order to elucidate the observed variations in σ_{dc} and E_{dc}, impedance spectroscopy and EPR studies have been carried out.

3.2. *Impedance spectroscopy*

The impedance spectra of all the investigated glasses depend considerably on their chemical composition. The characteristic features of these spectra follow the nature of conduction mechanism. The experimental spectra (complex impedance representation) can be classified into three types (i) single semicircle with a low frequency spur, (ii) spectra consisting of two depressed semicircles and (iii) single semicircle without spur [26]. The inclined straight line (spur) at the low frequency region could be the effect of mixed electrode and electrolyte interface. The magnitude of inclination in the straight line is related to the width of the relaxation time distribution [27]. The impedance spectra consisting of two semicircles represent mixed conduction while glasses exhibiting a single semicircle without spur are electronically conducting. Garbarczyk et al. [8] reported the simulated impedance spectra characteristic for ion conduction, mixed conduction and electronic conduction with the equivalent electrical circuits used to generate the spectra [8,28–30].

Conductance (G) and capacitance (C_p) were directly measured (for $x = 10$ mol%) from the impedance bridge and used to compute the real and imaginary parts of impedance using the relations given by Ross Macdonald [31]. Impedance plots of VBZ1 glass is shown in Fig. 5, which is used in dc conductivity determination. Values of Z' (bulk resistance) corresponding to the intersection of low frequency side of the high frequency arc were used for the purpose. The dc conductivity was calculated using Eq. (1) and the values lie in the range of 1.9×10^{-7}–1.1×10^{-5} S/cm (for $x = 10$ mol%). These values are comparable with those (measured using four-probe method) presented in Fig. 3. Impedance spectra of glass with $x = 20$ mol% showing two depressed semicircles, characteristic of mixed conduction are shown in Fig. 6. For $x \geq 30$ mol%, single semicircles without any spur are shown in Fig. 6 inset.

As can be seen from Fig. 4, isothermal conductivity at 313 K and activation energy (E_{dc}) varies nonlinearly with V_2O_5 mol%. This can be attributed to the enhanced interactions between polarons and mobile ions [29]. At lower $x = 10$ mol%, there is a reduction in the electronic component of conductivity due to the disruption of the glass network and the increased population of Li^+ ions. Eventually, there is

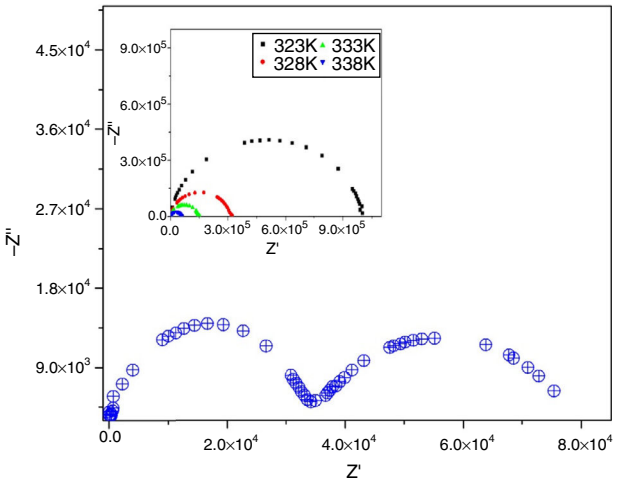

Fig. 6 – Impedance plot of VBZ 2 glass. Inset: Impedance plot of VBZ 3 (V_2O_5 rich) glass.

an enhanced population of Li^+ ions in the network structure compared to trapped polarons at x = 10 mol%. Thus, the ionic conductivity dominates. At x = 20 mol%, the interaction between electron and cation is maximum, suggesting a kind of transition from predominantly 'ionic' to 'electronic' conductivity. Hence, x = 20 mol% is considered to be the cross-over composition. In the present study, we identified two regimes viz. highly modified 'ion' conducting (x = 10 mol%) and least modified 'electronically' conducting regimes. As reported in the literature, alkali ion transport is characterized by high activation barrier [32]. Further, if electronic contribution to conductivity is significant as ionic contribution [1], then

$$\sigma_{total} = \sigma_{ionic} + \sigma_{electronic} \quad (3)$$

$$\log \sigma_{total} = \log(\sigma_{ionic} + \sigma_{electronic}) \quad (4)$$

$$\log \sigma_{total} = \log\left[\sigma_{ionic}\left(1 + \frac{\sigma_{electronic}}{\sigma_{ionic}}\right)\right] \quad (5)$$

$$\log \sigma_{total} \approx \log \sigma_0 - \frac{E_{ionic}}{kT} + \log\left(\frac{\sigma_{electronic}}{\sigma_{ionic}}\right) \quad (6)$$

the ratio $\sigma_{electronic}/\sigma_{ionic}$ varies from glass to glass, since $Li^+/([V^{4+}] + [V^{5+}]) = Li^+/V_{total} = r_c$ varies.

This ratio plays a pivotal role in non-linear variation of conductivity. A similar trend is seen in glasses containing both alkali oxide and TMO's [33–36]. The other possible explanation for the observed conductivity is that polaron percolation paths are blocked by alkali ions in alkali rich glasses [33–36]. More importantly modifier to network former ratio can be effective, it is a measure of disruption of the glass network. If the ratio is higher, the glass network becomes more depolymerized. In such a case the electron conduction paths are discontinuous [37]. In V_2O_5 rich glasses conductivity increases while the activation energy decreases (see Fig. 4). This can be well explained using Austin–Mott's relation [38]. Conductivity in such glasses is characterized by an electron transfer process represented by V^{4+}—O—V^{5+}. The increase in σ_{dc} with V_2O_5 concentration can be attributed to (i) a decrease in V—O—V distance resulting in a larger overlap of d-orbital wave functions and (ii) increase in the redox ratio, $C = [V^{4+}]/([V^{4+}] + [V^{5+}])$. The dependence of conductivity on composition is clearly reflected in EPR study.

3.3. *EPR spectroscopy*

EPR spectra of the investigated glasses are shown in Fig. 7. As can be seen from Fig. 7, a strong absorption line arises from the fact that at high V_2O_5 content, most of the vanadium ions are in the V^{4+} state. The absence of hyperfine structure (hfs) points to interaction between vanadium centers via V^{4+}—O—V^{5+} super-exchange mechanism. Generally, such glasses exhibit electronic conductivity [8]. However, the mechanism of conduction in glasses with high concentration of V_2O_5 has been suggested as the transfer of an electron from V^{4+} site to a V^{5+} site. Structural groups formed in V_2O_5 rich glasses, provide the path for the conduction of electrons [39]. The increase of the electronic conductivity in V_2O_5 rich glasses can be explained by considering the decrease in the average distance between the TMI sites. According to Mott's polaron theory, the dc conductivity rapidly varies with site

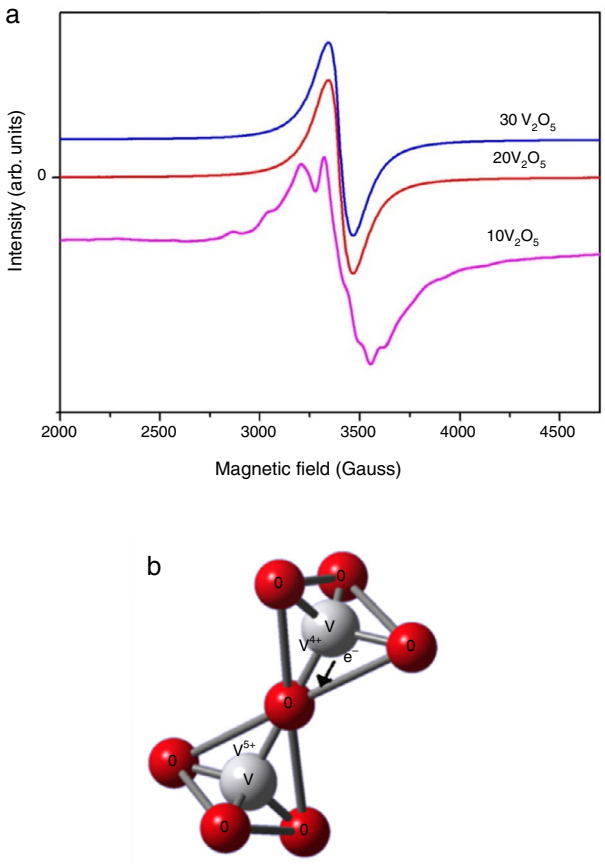

Fig. 7 – (a) EPR spectra of $xV_2O_5{\cdot}20Li_2O{\cdot}(80 - x)[0.6B_2O_3{:}0.4ZnO]$ glasses. (b) Schematic representation of electron hopping via V^{4+}—O—V^{5+} bonds.

spacing and redox ratio. The observed correlation between the concentration of V_2O_5 and the appearance of hyperfine structure (hfs) can be justified, taking into account that two nearest aliovalent vanadium centers can exchange an electron via bridging oxygen. The least modified network is characterized by a strongly cross-linked network. In such a network, the conditions for electron hopping via V^{4+}—O—V^{5+} bonds are more favorable than highly disrupted network. An illustration of transfer of electron from V^{4+} site to neighboring V^{5+} site is shown in Fig. 7b. At x = 20 mol%, the EPR spectra consists of V^{4+} line with a weak but visible superimposed hfs, which indicates the cross-over from non-hfs regime to hfs regime. A similar cross-over point is seen at this composition in the dc conductivity studies. Further, in highly modified glasses (x = 10 mol%) ion (Li^+) transport dominates the polaron conduction.

4. Conclusion

Lithium–zinc–boro-vanadate glasses were synthesized by microwave method by varying V_2O_5 concentration from 10 to 50 mol%. Glasses were characterized by XRD and DSC studies. As the concentration of V_2O_5 increases the T_g decreases suggesting that the rigidity of the network decreases while the fragility of glass itself increases. The dc conductivity study reveals a non-linear variation in conductivity and activation

energy. These nonlinearities are attributed to different conduction mechanisms due to the presence of both alkali oxide and TMO. Conductivity is predominantly ionic for glasses with low V_2O_5 content while predominantly electronic for glasses containing higher content of V_2O_5. Conductivity transition occurs at the concentrations of alkali ion and TMI are nearly equal.

Conflicts of interest

The authors declare no conflicts of interest.

Acknowledgement

The authors are grateful to Professor K.J. Rao, Solid State and Structural Chemistry Unit, Indian Institute of Science, Bangalore for encouragement and many helpful discussions.

REFERENCES

[1] Rao KJ. Structural chemistry of glasses. 1st ed. Amsterdam: Elsevier Science; 2002.
[2] Chethana BK, Narayana Reddy C, Rao KJ. Thermo-physical and structural studies of sodium zinc borovanadate glasses in the region of high concentration of modifier oxides. Mater Res Bull 2012;47:1810–20.
[3] Angell CA. Mobile ions in amorphous solids. Annu Rev Phys Chem 1992;43(1):693–717.
[4] Baskaran N, Govindaraj G, Narayanaswamy A. Solid-state batteries using silver-based glassy materials. J Power Sources 1995;55:153–7.
[5] Chandra A, Bhatt A, Chandra A. Ion conduction in superionic glassy electrolytes: an overview. J Mater Sci Technol 2013;29:193–208.
[6] Jozwiak P, Garbarczyk JE. Mixed electronic–ionic conductivity in the glasses of the Li_2O–V_2O_5–P_2O_5 system. Solid State Ionics 2005;176:2163–6.
[7] Abbas L, Bih L, Nadiri A, El Amraoui Y, Mezzane D, Elouadi B. Properties of mixed Li_2O and Na_2O molybdenum phosphate glasses. J Mol Struct 2007;876:194–8.
[8] Garbarczyk JE, Murawski P, Wasiucionek M, Tykarski L, Bacewicz R, Aleksiejuk A. Studies of silver–vanadate–phosphate glasses by Raman, EPR and impedance spectroscopy methods. Solid State Ionics 2000;136:1077–83.
[9] Narayana Reddy C, Veeranna Gowda VC, Chakradhar RPS. Elastic properties and structural studies on lead–boro–vanadate glasses. J Non-Cryst Solids 2008;354:32–40.
[10] Horopanitis EE, Perentzis G, Pavlidou E, Papadimitriou L. Electrical properties of lithiated boron oxide fast-ion conducting glasses. Ionics 2003;9:88–94.
[11] Das SS, Gupta CP, Srivatsava V. Ion transport studies in zinc/cadmium halide doped silver phosphate glasses. Ionics 2005;11:423–30.
[12] Kabi S, Ghosh A. Mixed glass former effect in AgI doped silver borophosphate glasses. Solid State Ionics 2014;262:778–81.
[13] Thangadurai V, Weppner W. Solid state lithium ion conductors: design considerations by thermodynamic approach. Ionics 2002;8:281–92.
[14] Mirzayi M, Hekmatshoar MH. Optical and IR study of Li_2O–CuO–P_2O_5 glasses. Ionics 2009;15:121–7.
[15] Mansour E, El-Egili K, El-Damrawi G. Ionic–polaronic behavior in CeO_2–PbO–B_2O_3 glasses. Physica B 2007;392:221–8.
[16] Subbalakshmi P, Veeraiah N. Study of CaO–WO_3–P_2O_5 glass system by dielectric properties, IR spectra and differential thermal analysis. J Non-Cryst Solids 2002;298:89–98.
[17] Muncaster R, Parke M. ESR spectra of glasses in the system V_2O_5–TeO_2. J Non-Cryst Solids 1977;24:399–412.
[18] Gupta S, Khanijo N, Mansingh A. The influence of V^{4+} ion concentration on the EPR spectra of vanadate glasses. J Non-Cryst Solids 1995;181:58–63.
[19] Sujatha B, Narayana Reddy C. Electrical switching behaviour in lead phosphovanadate glasses. Turk J Phys 2006;30:189–95.
[20] Venkata Subba Reddy M, Sudhakara Reddy M, Narayana Reddy C, Chakradhar RPS. Elastic properties of Na_2O–B_2O_3–V_2O_5 glasses. J Alloys Compd 2009;479:17–21.
[21] Moynihan CT. Correlation between the width of the glass transition region and the temperature dependence of the viscosity of high-Tg glasses. J Am Ceram Soc 1993;76:1081–7.
[22] Stavrou E, Kripotou S, Raptis C, Turrell S, Syassen K. Raman and DSC studies of fragility in tellurium-zinc oxide glass formers. Phys. Status Solidi C 2011;8(11–12):3039–42.
[23] Sujatha B, Narayana Reddy C, Chakradhar RPS. Dielectric relaxation and ion transport in silver–boro-tellurite glasses. Philos Mag 2010;90:2635–50.
[24] Languar A, Sdiri N, Elhouichet H, Ferid M. Conductivity and dielectric behavior of $NaPO_3$–ZnO–V_2O_5 glasses. J Alloys Compd 2014;590:380–7.
[25] Bhide A, Hariharan K. Sodium ion transport in $NaPO_3$–Na_2SO_4 glasses. Mater Chem Phys 2007;105:213–21.
[26] Jozwiak P, Garbarczyk JE, Wasiucionek M. Evaluation of transference numbers in mixed conductive lithium vanadate–phosphate glasses. Mater Sci Pol 2006;24:147–53.
[27] Barsoukov E, Macdonald JR. Impedance spectroscopy: theory, experiment, and applications. 2nd ed. New Jersey: Wiley Interscience; 2005.
[28] Garbarczyk JE, Wasiucionek M, Machowski P, Jakubowski W. Transition from ionic to electronic conduction in silver–vanadate–phosphate glasses. Solid State Ionics 1999;119:9–14.
[29] Krins N, Rulmont A, Grandjiean J, Gilbert B, Lepot L, Cloots R, et al. Structural and electrical properties of tellurovanadate glasses containing Li_2O. Solid State Ionics 2006;177:3147–50.
[30] Krasowski K, Garbarczyk JE. XRD, DSC, and admittance spectroscopy studies on some AgI–Ag_2O–V_2O_5 superionic glasses. Phys Status Solidi A 1996;158:K13–6.
[31] Macdonald JR. Impedance spectroscopy. Ann Biomed Eng 1992;20:289–305.
[32] Nagaraja N, Sankarappa T, Prashant Kumar M. Electrical conductivity studies in single and mixed alkali doped cobalt–borate glasses. J Non-Cryst Solids 2008;354:1503–8.
[33] Murawski L, Barcznski RJ. Electronic and ionic relaxations in oxide glasses. Solid State Ionics 2005;176:2145–51.
[34] Devidas GB, Sankarappa T, Chougule BK, Prasad G. DC conductivity in single and mixed alkali vanadophosphate glasses. J Non-Cryst Solids 2007;353:426–34.
[35] Ungureanu MC, Levy M, Souquet JL. Mixed conductivity of glasses in the P_2O_5–V_2O_5–Na_2O system. Ionics 1998;4:200–6.
[36] Barczynski RJ, Murawski I. Mixed electronic–ionic conductivity on vanadate oxide glasses containing alkaline ions. Mater Sci Pol 2006;24(1):221–7.
[37] Bacewicz R, Wasiucionek M, Twarog A, Filipowicz J, Jozwiak P, Garbarczyk JE. A XANES study of the valence state of vanadium in lithium vanadate phosphate glasses. J Mater Sci 2005;40:4267–70.
[38] Austin IG, Mott NF. Polarons in crystalline and non-crystalline materials. Adv Phys 1969;18:41–102.
[39] Doweidar H, Megahed A, Gohar IA. Mixed ionic–electronic conduction in sodium borate glasses with low V_2O_5 content. J Phys D: Appl Phys 1986;19:1939–46.